

# Identification of Three Novel Ring Expansion Metabolites of KAE609, a New Spiroindolone Agent for the Treatment of Malaria, in Rats, Dogs, and Humans<sup>§</sup>

Su-Er W. Huskey, Chun-qi Zhu, Melissa M. Lin,<sup>1</sup> Ry R. Forseth, Helen Gu, Oliver Simon, Fabian K. Eggimann, Matthias Kittelmann, Alexandre Luneau, Alexandra Vargas, Hongmei Li, Lai Wang, Heidi J. Einolf, Jin Zhang, Sarah Favara, Handan He, and James B. Mangold

*Drug Metabolism and Pharmacokinetics, Novartis Institutes for BioMedical Research, East Hanover, New Jersey (S.-E.W.H., C.Z., R.R.F., H.G., H.L., L.W., H.J.E., J.Z., S.F., H.H., J.B.M.); Technical Research and Development, Novartis Pharma, East Hanover, NJ (M.M.L.); Novartis Institute for Tropical Diseases, Singapore (O.S.); and Global Discovery Chemistry, Bioreactions Group, Novartis Institutes for BioMedical Research, Basel, Switzerland (F.K.E., M.K., A.L., A.V.)*

Received December 21, 2015; accepted February 19, 2016

## ABSTRACT

KAE609 [(1'*R*,3'*S*)-5,7'-dichloro-6'-fluoro-3'-methyl-2',3',4',9'-tetrahydrospiro[indoline-3,1'-pyridol[3,4-*b*]indol]-2-one] is a potent, fast-acting, schizonticidal agent being developed for the treatment of malaria. After oral dosing of KAE609 to rats and dogs, the major radioactive component in plasma was KAE609. An oxidative metabolite, M18, was the prominent metabolite in rat and dog plasma. KAE609 was well absorbed and extensively metabolized such that low levels of parent compound ( $\leq 11\%$  of the dose) were detected in feces. The elimination of KAE609 and metabolites was primarily mediated via biliary pathways ( $\geq 93\%$  of the dose) in the feces of rats and dogs. M37 and M23 were the major metabolites in rat and dog feces, respectively. Among the prominent metabolites of KAE609, the isobaric chemical species, M37, was observed, suggesting the involvement of an isomerization

or rearrangement during biotransformation. Subsequent structural elucidation of M37 revealed that KAE609, a spiroindolone, undergoes an unusual C-C bond cleavage, followed by a 1,2-acyl shift to form a ring expansion metabolite M37. The *in vitro* metabolism of KAE609 in hepatocytes was investigated to understand this novel biotransformation. The metabolism of KAE609 was qualitatively similar across the species studied; thus, further investigation was conducted using human recombinant cytochrome P450 enzymes. The ring expansion reaction was found to be primarily catalyzed by cytochrome P450 (CYP) 3A4 yielding M37. M37 was subsequently oxidized to M18 by CYP3A4 and hydroxylated to M23 primarily by CYP1A2. Interestingly, M37 was colorless, whereas M18 and M23 showed orange yellow color. The source of the color of M18 and M23 was attributed to their extended conjugated system of double bonds in the structures.

## Introduction

Malaria is one of the leading causes of death and disease worldwide, especially among young children in developing countries. Drug resistance to widely used artemisinin-based therapies (Carter et al., 2015; Hott et al., 2015) has become an imminent issue since drug-resistance strains were identified in Bangladesh, Cambodia, Thailand, Vietnam, Myanmar and Laos (Haque et al., 2013; Na-Bangchang and

Karbwang, 2013; Witkowski et al., 2013). Growing global efforts are focusing on finding new cures to combat malaria drug resistance.

KAE609 [(1'*R*,3'*S*)-5,7'-dichloro-6'-fluoro-3'-methyl-2',3',4',9'-tetrahydrospiro[indoline-3,1'-pyridol[3,4-*b*]indol]-2-one] (Fig. 1; Yeung et al., 2010), a spiroindolone, represents a new class of potent, fast-acting, schizonticidal agents for the treatment of malaria (Rottmann et al., 2010; Meister et al., 2011; Spillman et al., 2013). More recently, KAE609 was shown to be safe and well tolerated in healthy subjects up to a single dose of 300 mg and multiple doses of 150 mg daily for 3 days (Leong et al., 2014). Evaluation in 21 adult patients with uncomplicated malaria due to either *Plasmodium vivax* ( $n = 10$ ) or *Plasmodium falciparum* ( $n = 11$ ) showed that once-daily dosing of KAE609 at 30 mg for 3 days resulted in a rapid median parasite clearance time of approximately 12 hours for both *P. vivax* and *P. falciparum* (White et al., 2014).

In preparation for the clinical investigations described above, efforts were undertaken to understand *in vitro* metabolism of KAE609 across

All authors are employees of Novartis. The authors have no other relevant affiliations or financial involvement with any other organization or entity with a financial interest in or financial conflict with the subject matter or materials discussed in the manuscript apart from those disclosed. No writing assistance was utilized in the production of this manuscript.

<sup>1</sup>Current affiliation: Merck Research Laboratories, Rahway, NJ

[dx.doi.org/10.1124/dmd.115.069112](http://dx.doi.org/10.1124/dmd.115.069112).

§ This article has supplemental material available at [dmd.aspetjournals.org](http://dmd.aspetjournals.org).

**ABBREVIATIONS:** ADME, absorption, distribution, metabolism, and excretion; AUC, area under concentration-time curve;  $\beta$ -RAM, online radioactivity monitor; COSY, correlation spectroscopy; CYP, cytochrome P450; DPM, disintegration per minute; DQF-COSY, double quantum filter correlation spectroscopy; H/D, hydrogen/deuterium; HMBC, heteronuclear multiple bond correlation; HPLC, high-performance liquid chromatography; KAE579, (1'*R*,3'*S*)-5-chloro-6'-fluoro-3'-methyl-2',3',4',9'-tetrahydrospiro[indoline-3,1'-pyridol[3,4-*b*]indol]-2-one; KAE609, (1'*R*,3'*S*)-5,7'-dichloro-6'-fluoro-3'-methyl-2',3',4',9'-tetrahydrospiro[indoline-3,1'-pyridol[3,4-*b*]indol]-2-one; LC-MS/MS, liquid chromatography-tandem mass spectrometry; MS, mass spectrometry; MS<sup>E</sup>, MS technique involving dynamic collision between high and low energy switching; *m/z*, mass-to-charge ratio; NMR, nuclear magnetic resonance; %PRA, percentage of radioactivity; PK, pharmacokinetics; QC, quality control;  $t_{1/2}$ , terminal elimination half-life.

species as well as absorption, distribution metabolism, and excretion (ADME) of KAE609 in preclinical species. Following oral dosing, KAE609 was the major component in plasma. An oxidative metabolite, M18, was the major metabolite in rat and dog plasma, while M37 and M23 were the major metabolites in rat and dog feces, respectively. To note, nomenclature of metabolites was based on their high-performance liquid chromatography (HPLC) elution time in the study in which they were first identified. Based on liquid chromatography–tandem mass spectrometry (LC-MS/MS) analysis, M37 shared the same molecular weight with KAE609, suggesting that M37 was a product of isomerization or rearrangement of KAE609 during biotransformation. Therefore, the structural elucidation of M37 was undertaken to facilitate the understanding of this unusual biotransformation. During purification of M37 from rat feces, two brightly colored yellow fractions were identified corresponding to M18 and M23. The strategies and approaches we used in the elucidation of structures of M18 and M23 and the metabolic pathways of KAE609 are described herein.

In parallel to the *in vivo* studies above, *in vitro* across-species metabolism of KAE609 revealed that M23 was a prominent metabolite in human hepatocytes. Based on the preclinical ADME studies, M23 was not detected in rat or dog plasma, although M23 was the major metabolite in dog excreta. In view of Metabolites in Safety Testing and International Conference on Harmonisation guidance (Baillie et al., 2002; Baillie, 2008; Smith and Obach, 2009; U.S. Food and Drug Administration 2008, 2010, and 2012 guidance, available at <http://www.fda.gov/cder/guidance/index.htm> and <http://www.fda.gov/Drugs/GuidanceComplianceRegulatoryInformation/Guidances/default.htm>), we describe herein the strategy we used regarding the potential exposure coverage of M23 in humans.

In this article, we describe the strategies and approaches used in the structural elucidation of three key metabolites of KAE609, investigation of the cytochrome P450 (CYP) enzymes involved in a novel ring expansion reaction of KAE609 to generate metabolite M37 and subsequent formation of oxidative highly colored metabolites from M37. To the best of our knowledge, this is the first report that revealed the ring expansion of a spiroindolone and generation of two colored metabolites (M18 and M23) from a colorless precursor metabolite (M37) by a single CYP-catalyzed oxidation reaction. All these three metabolites (M37, M18, and M23) showed no pharmacological activity after the spiroindolone core of KAE609 was lost by biotransformation.

## Materials and Methods

### Chemicals

KAE609, KAE579 [(1' *R*,3'*S*)-5-chloro-6'-fluoro-3'-methyl-2',3',4',9'-tetrahydrospiro[indoline-3,1'-pyridol[3,4-*b*]indol]-2-one], compound 1 (M37), compound 2 (M18), and compound 3 (M23) were synthesized by Novartis Institute for Tropical Diseases and compound 3 (M23) was also prepared by the Novartis Global Discovery Chemistry Bioreactions Group. [<sup>14</sup>C]KAE609 was prepared by Novartis Isotope laboratories and radiochemical purity was > 99%.

Microsomal preparations from baculovirus-infected insect cells expressing recombinant human CYP enzymes coexpressed with CYP oxidoreductase [CYP1A1, CYP1A2, CYP1B1, CYP2C18, CYP2D6, CYP3A5, or CYP4A11], recombinant human CYP enzymes coexpressed with CYP oxidoreductase and cytochrome *b*<sub>5</sub> [CYP2A6, CYP2B6, CYP2C8, CYP2C9 (Arg<sub>144</sub>,Ile<sub>359</sub>), CYP2C19, CYP2E1, CYP2J2, CYP3A4, CYP4F2, CYP4F3A, CYP4F3B or CYP4F12], as well as control microsomes were purchased from Corning Discovery Labware (Corning, NY). Hepatocyte culture plates were obtained from Corning Incorporated (Corning, NY). Krebs-Henseleit maintenance medium,  $\beta$ -NADPH, dimethylsulfoxide, potassium phosphate (mono- and dibasic), MgCl<sub>2</sub>, sodium bicarbonate, fructose, glycine, acetonitrile, methanol, ammonium formate, and formic acid were purchased from Sigma-Aldrich (St. Louis, MO). OPTI-FLUOR liquid scintillant was purchased from Packard

(Downers Grove, IL). Control blank plasma samples from rats and dogs were purchased from Bioreclamation (Hicksville, NY).

### Chemical Synthesis of Metabolites

Chemical synthesis of M37 (compound 1), M18 (compound 2), and M23 (compound 3) was carried out for structural confirmation and additional biologic profiling. A detailed description of the preparation and characterization of the metabolites can be found in the Supplemental Materials and Methods.

### Biocatalytic Synthesis of Compound 3 (M23)

**Preparation of Biocatalyst.** The biocatalyst, *Escherichia coli* expressing recombinant human CYP1A2, was prepared as described in Kittelmann et al. (2012).

**Biotransformation, Preparative Conditions (Compound 3, M23).** In a 400-ml polyethylene flask, 40 ml cell suspension (optical density at 600 nm = 100) in PSE buffer (potassium phosphate 50 mM, sucrose 250 mM, and EDTA 0.25 mM, pH 7.5) was mixed with 10 ml 0.9% NaCl solution and 5 ml nutrient solution (40 g/l glucose, 40 g/l lactose, and 60 g/l aqueous sodium citrate). The biotransformation was initiated by adding the substrate solution, containing 2 mg compound 2 (M18) dissolved in 2.5 ml acetonitrile. The reaction was incubated with open cap at 30°C and 250 rpm for 16 hours in an orbital shaker.

**Purification of Biotransformation Product (Compound 3).** After incubation, the reaction was mixed with 5 g sodium chloride and extracted three times with 100 ml ethyl acetate. The combined organic layers were mixed and evaporated to dryness under reduced pressure. The residual raw product was dissolved in 3 ml acetonitrile and injected into a 250 × 10 mm Nucloeodur 100-10 C18 ec column (Macherey-Nagel, Düren, Germany). The conditions for preparative HPLC were as follows: solvent A, 0.05% trifluoroacetic acid in water; solvent B, acetonitrile; gradient, 0–5 minutes 10% B, 5–48 minutes 10%–95% B, 48–53 minutes 100% B; flow rate, 4.5 ml/min; room temperature; UV detection, 320 nm; and fraction size, 2 ml. The product eluted between 40% and 50% B. The product containing fractions were combined and dried by Speedvac lyophilization overnight. The product (1 mg) was obtained with > 95% purity (HPLC/full diode array detector) and analyzed by nuclear magnetic resonance (NMR) spectroscopy. The isolated yield was 46%.

### In Vitro Incubations

To identify the CYP enzyme(s) involved in the metabolism of KAE609 or M18 (compound 2) in humans, test compound (44  $\mu$ M [<sup>14</sup>C]KAE609 or 50  $\mu$ M compound 2) was incubated with 19 commercially available recombinant human CYP enzymes (listed in the chemicals section), or control microsomes in 100 mM potassium phosphate buffer (pH 7.4) containing 5 mM MgCl<sub>2</sub>. The reactions were thermoequilibrated for 3 minutes at 37°C and initiated by the addition of 1 mM  $\beta$ -NADPH. The reactions were incubated for 30 minutes at 37°C and were quenched by the addition of an equal volume of cold acetonitrile. After vortex mixing and centrifugation, an aliquot of each sample was analyzed by LC-MS/MS.

### Animals

Male Wistar Hannover rats (approximately 227–310 g, *n* = 12) were purchased from Harlan Laboratories (South Easton, MA). Catheters were surgically implanted into the carotid artery and/or jugular vein of rats by the vendor (only one catheter was implanted into carotid artery for blood collection from rats receiving the oral dose). All rats were housed individually in Culex metabolism cages (Culex Autosampler; BAS, Indianapolis, IN) in a temperature- and humidity-controlled room (22 ± 2°C; 50% ± 15%) with free access to food and water (food was withheld until 4 hours postdose).

Male beagles (approximately 10–14 kg, *n* = 5) were purchased from Marshall farms (North Rose, NY) and kept in animal facility at Novartis for pharmacokinetics (PK) and ADME studies. The dogs were housed individually in a temperature- and humidity-controlled room. Dogs were acclimated to the metabolism cages 1 night prior to dosing. Dogs had free access to water and were given food once daily (food was withheld until 2 hours postdose).

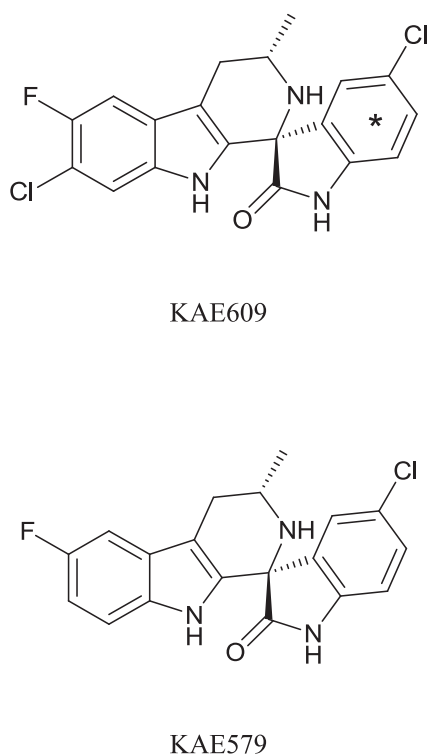


**Fig. 1.** Structure of KAE609 and KAE579. KAE609 is uniformly labeled in phenyl ring (indicated by asterisk). KAE579, a derivative of KAE609, was used as an internal standard for the quantification of KAE609.

#### Dose Administration

All doses were based on the individual body weights of animals on the day of dosing. [ $^{14}\text{C}$ ]KAE609 (specific activity 40  $\mu\text{Ci}/\text{mg}$  at 5 mg/kg for rats; and 50  $\mu\text{Ci}/\text{mg}$  at 1 mg/kg for dogs) was dissolved in ethanol, polyethylene glycol (PEG300) and pluronic F68 (5% in water) [10:20:70 (v/v/v)] for intravenous dosing. [ $^{14}\text{C}$ ]KAE609 (specific activity 20  $\mu\text{Ci}/\text{mg}$  at 10 mg/kg) was prepared in solution containing 1 N HCl (0.28%), solutol HS 15 (5%), and 50 mM citrate buffer, pH 3 (94.7%) for oral dosing to rats. [ $^{14}\text{C}$ ]KAE609 (specific activity 16.7  $\mu\text{Ci}/\text{mg}$  at 3 mg/kg) was prepared in suspension containing 0.5% (w/v) methyl cellulose and 2% solutol HS 15 in water for oral dosing to dogs.

Each rat received an intravenous bolus injection via the jugular vein cannula. Each dog received an intravenous slow bolus injection via the cephalic vein. The oral dose was administered by gavage in both rats and dogs.

#### Blood Collection

Blood samples (200  $\mu\text{l}$ ) were collected from the carotid artery of rats at selected time intervals in Culex tubes. Saline (200  $\mu\text{l}$ ) was automatically injected after sample was collected to clear the cannula and replace the volume of blood samples. Blood samples were collected via catheters placed in the cephalic vein of each dog at selected time intervals. The total blood volume collected did not exceed 1% of the body weights of rats and dogs.

#### Urine and Feces Collection

Urine and feces were collected daily from each of the animals for 7 days. Up to 3 days, the urine collection tubes were cooled with ice. After the final collection, each cage was rinsed with water followed by 50% methanol. The cage wash was assayed for radioactivity. Urine and feces samples were stored at  $-20^\circ\text{C}$  until analysis.

#### Sample Preparation

The plasma was obtained by centrifugation of blood samples at  $4^\circ\text{C}$  (2000  $\times$  g) for 10 minutes. An aliquot of each blood sample was used for radioactivity analysis (see the sample analysis section). An aliquot of plasma sample was

counted directly for radioactivity. The remaining plasma samples were stored at  $-20^\circ\text{C}$  until analysis.

#### Plasma for the Quantification of KAE609

Blank plasma and study samples were thawed at room temperature. Standards and quality control (QC) samples were prepared on the day of analysis by adding appropriate standard or QC (25  $\mu\text{l}$ ) spiking solution to 475  $\mu\text{l}$  blank plasma. Samples were loaded using a protein precipitation plate, which was attached above a 1-ml 96-well assay plate. An aliquot (25  $\mu\text{l}$ ) of study samples, blanks, standards, or QC samples was added to the appropriate well followed by the addition of acetonitrile (100  $\mu\text{l}$ ) and the internal standard (KAE579; 25  $\mu\text{l}$ , 500 ng/ml) to each well. Samples were mixed for 5 minutes and centrifuged at 2500 rpm for 15 minutes at  $25^\circ\text{C}$ . The filtrate was evaporated to dryness at approximately  $45^\circ\text{C}$  under a stream of nitrogen (TurboVap LV; Zymark Corp., Taunton, MA). The residues were reconstituted with 300  $\mu\text{l}$  acetonitrile/water/formic acid [10:90:0.1 (v/v/v)]. An aliquot (10  $\mu\text{l}$ ) was analyzed for KAE609 and KAE579 by LC-MS/MS.

#### Plasma and Fecal Homogenates for Metabolic Profiling of KAE609

All plasma samples were thawed at room temperature and a 150- $\mu\text{l}$  aliquot was pooled from each animal at each time point. Each plasma pool was diluted with 250  $\mu\text{l}$  water and extracted with 2 ml acetonitrile/methanol/acetic acid [50:50:0.1 (v/v/v)]. Fecal samples (5% and 1% by weight from rat and dog feces, respectively) were pooled from fecal homogenate prepared from rats during 0–96 hours postdose and from dogs 0–72 hours postdose. The resulting pooled fecal samples were extracted three times with 3 volumes of acetonitrile/methanol/acetic acid [50:50:0.1 (v/v/v)].

After centrifugation at 3500  $\times$  rpm for 10 minutes, the supernatants were combined and concentrated under a stream of nitrogen. Residues were reconstituted with acetonitrile/deionized water [50/50 (v/v)]. The recoveries of radioactivity were 63.4% (i.v.) and 64.1% (oral) from rat feces and 60.7% (i.v.) and 66.7% (oral) from dog feces, respectively.

#### Sample Analysis

**Determination of Radioactivity.** The radioactivity of all samples was determined by liquid scintillation counting. For quench correction, an external standard ratio method was used. Quench correction curves were established by means of sealed standards. An aliquot of plasma and urine samples were counted directly for radioactivity.

Solvable (500  $\mu\text{l}$ ) was added to each blood sample and incubated in a shaking water bath at  $50^\circ\text{C}$  for 2 hours. After incubation, 50  $\mu\text{l}$  100 mM EDTA as an antifoaming agent and 200  $\mu\text{l}$  30% hydrogen peroxide were added to decolorize the samples. The sample vials were loosely capped and returned to the water bath for 3 hours. Thereafter, 10 ml Eq. 989 scintillation cocktail was added and the samples were placed in the dark overnight to reduce chemiluminescence prior to counting for radioactivity.

Fecal samples from animals were homogenized with 2 or 3 volumes of water. Duplicate samples (approximately 100 mg) of the slurry were weighed into scintillation vials and processed as described above for blood samples prior to radioactivity determination. The remaining fecal homogenate was stored frozen at  $-20^\circ\text{C}$  until LC-MS/MS analysis.

**Quantification of KAE609 by LC-MS/MS.** Samples were analyzed on an LC-MS/MS system consisting of a Shimadzu HPLC system (Shimadzu, Kyoto, Japan) and Sciex API4000 mass spectrometer using Analyst software version 1.4.2 (AB Sciex, Foster City, CA). The mass spectrometer was operated in the positive ion mode, using turbospray ionization, with a source temperature of  $425^\circ\text{C}$ . Chromatographic separation was carried out on a Mac-Mod Analytical ACE 5 C8 50  $\times$  2.1 mm column. KAE609 and the internal standard (KAE579, Fig. 1) were eluted using a gradient method with a mobile phase consisting of the following: A, water containing 0.1% formic acid; and B, acetonitrile containing 0.1% formic acid. The gradient was 35% B for 0.5 minutes, increased to 90% B from 0.5 to 2 minutes, followed by a 1-minute hold at 90%B. The multiple reaction monitoring transitions for KAE609 and KAE579 had a mass-to-charge ratio ( $m/z$ ) of 390.2 to  $m/z$  347.1 and  $m/z$  356.2 to  $m/z$  313.1, respectively.

Calibration curves were generated by plotting the respective peak area ratios (y) of KAE609 to the internal standard versus the concentrations (x) of the

calibration standards using weighted  $1/x^2$  quadratic least-squares regression. The quantification was performed using Analyst software and Watson LIMS version 7.2.0.01 (Thermo Scientific, Philadelphia, PA). Concentrations in QC and study samples were calculated from the resulting peak area ratios and interpolation from the regression equations of the calibration curves. The lower limit of quantification was 1.0 ng/ml.

**Metabolic Profiling by LC-MS/MS.** Metabolic profiling was performed on a Waters Acquity UPLC System (Waters Corp., Milford, MA), equipped with an autosampler and a quaternary pump, and an online radioactivity monitor ( $\beta$ -RAM) or a fraction collector. Chromatographic separation was carried out on a Mac-Mod Analytical Zorbax SB-C18  $150 \times 3.0$  mm,  $3.5\text{-}\mu\text{m}$  column. KAE609 and the metabolites were eluted using a linear gradient method with a mobile phase consisting of the following: A, 5 mM ammonium acetate containing 0.1% formic acid; and B, acetonitrile/methanol [1:1 (v/v)] containing 0.1% formic acid. The gradient was 5% B for 5 minutes, increased to 50% B from 5 to 12 minutes, increased to 60% B from 12 to 30 minutes, increased to 75% B from 30 to 40 minutes, increased to 85% B from 40 to 45 minutes, and increased to 98% B from 45 to 50 minutes, followed by a 3-minute hold at 98% B.

The HPLC column eluent was split 1:4 [mass spectrometry (MS)/fraction collector or MS/ $\beta$ -RAM]. The eluent from the fraction collector was mixed with methanol (0.5 ml/min) and collected directly into 96-Deepwell LumaPlates coated with solid scintillant at 0.15 minutes per well using a fraction collector. The plates were dried at  $40^\circ\text{C}$  under a stream of nitrogen. The plates were counted for 10–15 minutes per well in a TopCount Model NXT radioactivity detector. Online monitoring with  $\beta$ -RAM employed a  $250\text{-}\mu\text{l}$  liquid cell and eluent was mixed with 1 ml/min IN-Flow 2:1 (IN/US Systems, Tampa, FL) liquid scintillant. The resulting data were processed using the Laura Data System (version 4.0; LabLogic Systems Inc., Brandon, FL). All quantification was based on the radioactivity associated with the chromatographic peaks.

**Online Hydrogen/Deuterium Exchange LC/MS-MS Method.** Hydrogen/deuterium (H/D) exchange LC/MS experiments were conducted. In these experiments, water was substituted with deuterium oxide ( $\text{D}_2\text{O}$ ) in the HPLC mobile phase (A: 5 mM ammonium formate in  $\text{D}_2\text{O}$  containing 0.1% formic acid). Samples were analyzed under the identical LC-MS/MS method, as described below.

**LC-MS Instrumentation and Operating Conditions.** The structural characterization of metabolites was carried out using the above HPLC profiling method coupled to a two-channel Z-spray (LockSpray) Waters Synapt G2S quadrupole time-of-flight mass spectrometer. The Q-TOF Synapt was operated in V-mode with a typical resolving power of at least 10,000. Qualitative analyses were carried out using electrospray ionization in the positive ionization mode using a lock spray source. Leucine enkephalin was used as the mass reference standard for exact mass measurements and was delivered via the second spray channel at a flow rate of  $20\ \mu\text{l}/\text{min}$ . Accurate mass LC/MS data were collected in an alternating low-energy (MS) and elevated-energy ( $\text{MS}^E$ ) mode of acquisition. In low-energy MS mode, data were collected at consistent collision energy of 2 eV. In elevated  $\text{MS}^E$  mode, collision energy was ramped from 15 to 30 eV during data collection cycle.

**NMR Analysis of M37, M18, and M23.** Detailed description of procedures for the isolation of metabolites from rat fecal extract can be found in the Supplemental Materials and Methods.  $^1\text{H}$  spectra were acquired for M37, M18, and M23 (dissolved in acetonitrile- $d_3$ ) as well as reference compounds 1, 2, and 3 (approximately  $100\ \mu\text{g}$ , dissolved in acetonitrile- $d_3$ ). Selective nuclear Overhauser effect spectroscopy data were acquired for M37 using a mixing time of 0.4 seconds, 32k data point collection over a spectral width of 12,019 Hz, and 2048 scans. A line broadening factor of 1 Hz was applied to the free induction decay data before Fourier transformation. The double quantum filter correlation spectroscopy (DQF-COSY) spectrum was acquired for M23. NMR spectra were acquired on a Bruker DRX600 MHz spectrometer equipped with a 3-mm dual CryoProbe at 300 K. For the DQF-COSY spectrum, the  $90^\circ$  pulse (P1) was calibrated at a  $^1\text{H}$  transmitter power of 0.2 dB, and the following acquisition parameters were used: acquisition time, 0.7 seconds; complex increments, 1024; and number of scans, 64. Spectra were processed in MestReNova. DQF-COSY spectra were processed using 8k (f2) by 2k (f1) zero filling. Window functions were applied to the raw free induction decay (f2, sine bell; f1, square sine function).

## Data Processing

**Quantification of KAE609 and Metabolites by Radiometry.** KAE609 and metabolites were quantified in the extracts by radiochromatography. Peaks were selected visually from the radiochromatogram, and their corresponding areas were determined via peak integration (LAURA laboratory software from LabLogic).

The percentage of radioactivity (%PRA) in a particular peak, Z, was calculated as follows:

$$\%PRA \text{ in } Z = \frac{\text{DPM in peak } Z}{\text{total DPM in all integrated peaks}} \times 100$$

Where DPM is disintegration per minute. The concentration or amount of each component was calculated as %PRA (as a fraction) multiplied by the total concentration (nanogram equivalent per milliliter) or percent of dose in the excreta.

**Pharmacokinetic Parameters.** The pharmacokinetic parameters were calculated using actual recorded sampling times and noncompartmental method(s) with Phoenix (WinNonlin version 6.2; Pharsight, Certara L.P., Princeton, NJ). Concentrations below the lower limit of quantification were treated as zero for PK parameter calculations. The linear trapezoidal rule was used for area under concentration-time curve (AUC) calculation. Regression analysis of the terminal plasma elimination phase for the determination of terminal elimination half-life ( $t_{1/2}$ ) included at least three data points after  $C_{\text{max}}$ . If the adjusted  $R^2$  value of the regression analysis of the terminal phase was less than 0.75, no values were reported for  $t_{1/2}$ ,  $\text{AUC}_{\text{inf}}$ ,  $V_z/F$ , and clearance/F.

## Results

### Mass Balance and PK of KAE609 in Rats and Dogs

After intravenous or oral dosing of [ $^{14}\text{C}$ ]KAE609, mass balance was achieved in both rats and dogs, with 93%–100% of the administered radioactivity dose being recovered in feces and < 2% of the dose being recovered in urine. KAE609 had a long  $t_{1/2}$  (8.2 hours in rats and 10.9 hours in dogs), low plasma clearance (0.252 l/h per kilogram in rats and 0.201 l/h per kilogram in dogs), and moderate volume of distribution at steady state (3.18 l/kg in rats and 2.17 l/kg in dogs). After oral dosing, KAE609 was slowly absorbed in rats, with a  $C_{\text{max}}$  of 1210 ng/ml observed at 5.3 hours ( $t_{\text{max}}$ ); however, it was relatively rapidly absorbed in dogs, with a  $C_{\text{max}}$  of 868 ng/ml observed at 1.7 hours ( $t_{\text{max}}$ ). The extent of oral absorption was complete in rats and it was estimated to be 72.5% in dogs. The estimated oral bioavailability was 84.6% in rats and 67.7% in dogs, indicating a minimal first-pass effect in both rats and dogs. Detailed summary tables of mass balance and PK parameters can be found in the Supplemental Tables 1 and 2.

### Metabolite Profiling of [ $^{14}\text{C}$ ]KAE609 in Rat and Dog Plasma

After intravenous or oral dosing, the major radiolabeled component in rat and dog plasma was KAE609, accounting for approximately 75%–84% of the total radioactivity AUC by either dosing route. The prominent metabolite was M18, accounting for approximately 10%–19% of total radioactivity AUC by either dosing route. Several minor metabolites were also detected, each accounting for  $\leq 3\%$  of total radioactivity AUC by either dosing route. Detailed graphic presentations can be found in the Supplemental Figs. 1 and 2.

### Metabolite Profiling of [ $^{14}\text{C}$ ]KAE609 in Rat and Dog Feces

KAE609 was well absorbed and extensively metabolized in rats and dogs, such that unchanged KAE609 accounted for approximately 10%–11% of the dose in rat feces and KAE609 was not detected in dog feces by either dosing route (Fig. 2). M37 was the major component in rat feces, accounting for approximately 23%–26% of the intravenous or oral dose, whereas M23 was the major metabolite, accounting for

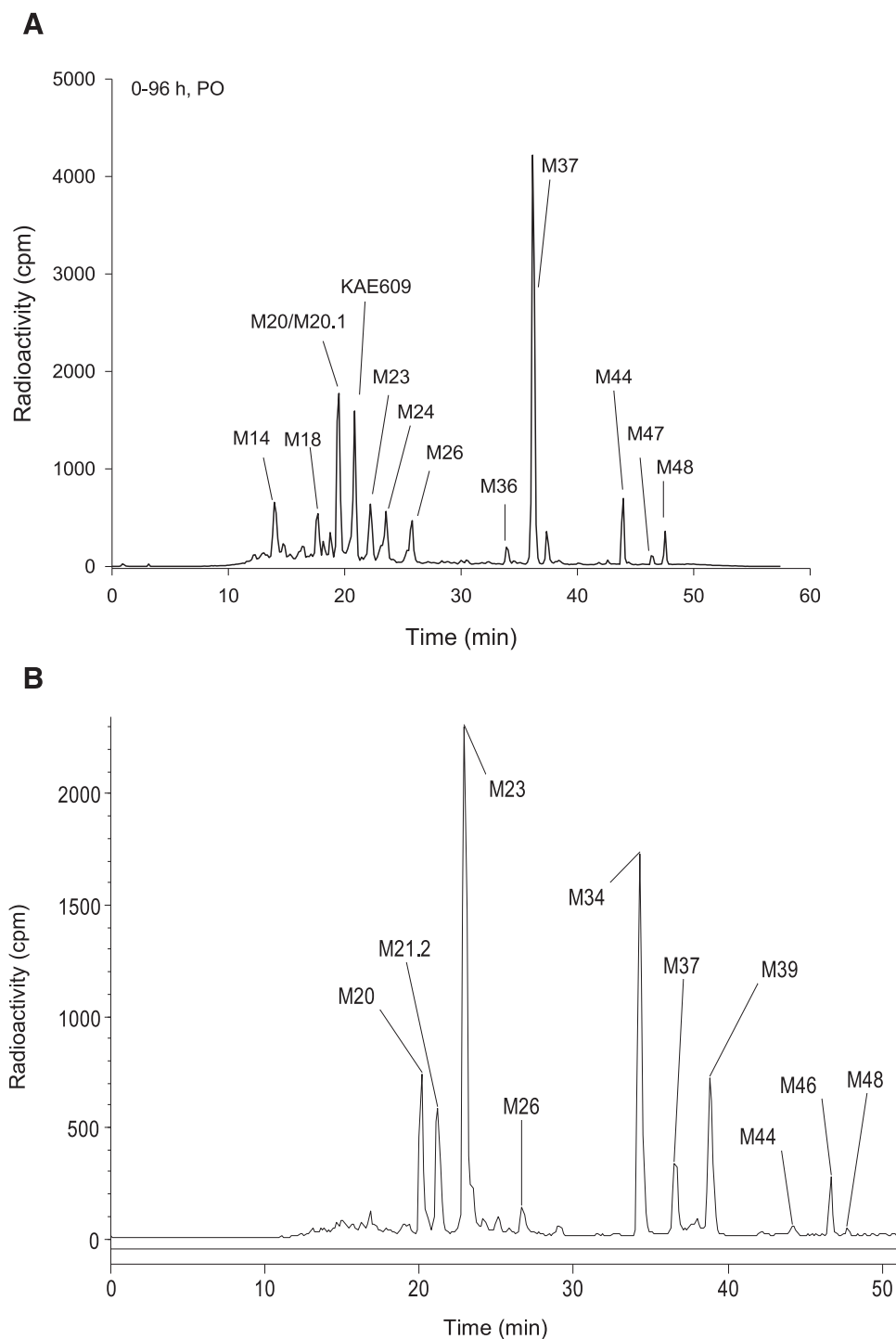


**Fig. 2.** Representative metabolic profiles in pooled rat feces (A) and pooled dog feces (B) after oral dosing of [ $^{14}\text{C}$ ]KAE609. Feces samples were collected daily from animals up to 7 days. After homogenization, fecal homogenates were extracted and analyzed by LC-MS/MS. The HPLC separation of KAE609 and metabolites was performed, as described in the *Materials and Methods*. PO, oral administration.

approximately 25%–30% of either the intravenous or oral dose. In rat feces, several metabolites (M14, M18, M23, M24, M26, M36, M44, M47, and M48) were identified, each accounting for approximately 2%–8% of the dose. Two metabolites (M20 and M20.1) were not separated under the HPLC condition used in this study, together accounting for approximately 12%–13% of the dose by either dosing route. In dog feces, several prominent metabolites (M20, M21.2, M34, and M39), each accounting for approximately 10%–20% of the dose, and several minor metabolites (M26, M37, M44, M46, and M46), each accounting for approximately 4%–6% of the dose, were identified.

Only 1%–2% of the intravenous and oral doses were recovered in urine from either rats or dogs during the period of 0–168 hours; therefore, urine was not analyzed for metabolite profile.

#### Structural Characterization of [ $^{14}\text{C}$ ]KAE609 and M37 by LC-MS/MS and NMR

The structures of the metabolites were proposed based on their elemental composition derived from accurate mass measurements (<3–5 ppm), fragment ions in their data-dependent MS<sup>2</sup> and MS<sup>3</sup> mass spectra, and exchangeable hydrogen atoms in the H/D exchange

TABLE 1

Fragmentation patterns of KAE609 and metabolites

Structural characterization of metabolites was carried out by LC-MS/MS analysis with accurate mass measurements. The proposed structures of the metabolites were based on their elemental composition derived from accurate mass measurements and fragment ions in their data-dependent MS<sup>2</sup> and MS<sup>3</sup> mass spectra. Comparison of metabolite fragment ions with those of KAE609 allowed the assignment of regions of biotransformation.

Compound	[MH <sup>+</sup> ] <i>m/z</i>	Elemental Formula	Diagnostic Fragment Ions
KAE609	390.0573	C <sub>19</sub> H <sub>15</sub> Cl <sub>2</sub> FN <sub>3</sub> O	390, 347, <sup>a</sup> 319, <sup>a</sup> 311, 312, 284, 276
M14	404.0362	C <sub>19</sub> H <sub>13</sub> Cl <sub>2</sub> FN <sub>3</sub> O <sub>2</sub>	404, 386, <sup>a</sup> 360, 351, 325, 278
M18	388.0416	C <sub>19</sub> H <sub>13</sub> Cl <sub>2</sub> FN <sub>3</sub> O	388, 359, <sup>a</sup> 324
M20	404.0375	C <sub>19</sub> H <sub>13</sub> Cl <sub>2</sub> FN <sub>3</sub> O <sub>2</sub>	404, <sup>a</sup> 375, 340
M20.1	388.0425	C <sub>19</sub> H <sub>13</sub> Cl <sub>2</sub> FN <sub>3</sub> O	388, 360, <sup>a</sup> 324
M21.2	404.0375	C <sub>19</sub> H <sub>13</sub> Cl <sub>2</sub> FN <sub>3</sub> O <sub>2</sub>	404, <sup>a</sup> 375, <sup>a</sup> 368, <sup>a</sup> 340, <sup>a</sup> 312
M23	404.0363	C <sub>19</sub> H <sub>13</sub> Cl <sub>2</sub> FN <sub>3</sub> O <sub>2</sub>	404, 375, 340, 235
M24	404.0362	C <sub>19</sub> H <sub>13</sub> Cl <sub>2</sub> FN <sub>3</sub> O <sub>2</sub>	404, 375, 340, 235
M26	406.0515	C <sub>19</sub> H <sub>15</sub> Cl <sub>2</sub> FN <sub>3</sub> O <sub>2</sub>	406, <sup>a</sup> 373, 327, 226 <sup>a</sup>
M34	406.0528	C <sub>19</sub> H <sub>15</sub> Cl <sub>2</sub> FN <sub>3</sub> O <sub>2</sub>	406, 373, <sup>a</sup> 355, <sup>a</sup> 309, <sup>a</sup> 210 <sup>a</sup>
M36	404.0042	C <sub>19</sub> H <sub>13</sub> Cl <sub>2</sub> FN <sub>3</sub> O <sub>2</sub>	404, <sup>a</sup> 375
M37	390.0579	C <sub>19</sub> H <sub>13</sub> Cl <sub>2</sub> FN <sub>3</sub> O	390, 373, 210, <sup>a</sup> 175
M39	404.037	C <sub>19</sub> H <sub>13</sub> Cl <sub>2</sub> FN <sub>3</sub> O <sub>2</sub>	404, 355, <sup>a</sup> 337, <sup>a</sup> 319
M40	388.0419	C <sub>19</sub> H <sub>13</sub> Cl <sub>2</sub> FN <sub>3</sub> O	388, <sup>a</sup> 359, 324, 210
M44	402.0223	C <sub>19</sub> H <sub>11</sub> Cl <sub>2</sub> FN <sub>3</sub> O <sub>2</sub>	402, <sup>a</sup> 339, 325, 197, <sup>a</sup> 172
M46	402.0209	C <sub>19</sub> H <sub>11</sub> Cl <sub>2</sub> FN <sub>3</sub> O <sub>2</sub>	402, <sup>a</sup> 310, 276, 172
M47	401.9908	C <sub>19</sub> H <sub>11</sub> Cl <sub>2</sub> FN <sub>3</sub> O <sub>2</sub>	402, <sup>a</sup> 367, 310
M48	386.0256	C <sub>19</sub> H <sub>11</sub> Cl <sub>2</sub> FN <sub>3</sub> O	386, <sup>a</sup> 351, 323, 309

<sup>a</sup>Indicates the most abundant fragment ions.

experiment. The elemental formula and diagnostic fragmentation ions of KAE609 and metabolites are summarized in Table 1. Detailed product ion spectra of KAE609, M37, M18, and M23 can be found in Supplemental Figs. 3–6.

KAE609 ([MH]<sup>+</sup> = 390) contained two chlorine atoms with an isotope ratio of approximately 100:64 (<sup>35</sup>Cl:<sup>37</sup>Cl). The fragment ion at *m/z* 347 was formed from loss of the vinyl amine moiety. Further loss of the Cl radical from *m/z* 347 gave fragments at *m/z* 312, and loss of CO from *m/z* 312 gave fragments at *m/z* 284.

Comparison of metabolite fragment ions with those of KAE609 allowed the assignment of regions of biotransformation. The product ion spectrum of M37 ([MH]<sup>+</sup> = 390) showed fragment ions at *m/z* 210 (loss of chloro-dihydro-quinazolin-one). There were no obvious similar fragmentation patterns between KAE609 and M37, which made the assignment of M37 with only LC-MS/MS data not feasible.

In the H/D exchange experiment, the full-scan mass spectra of KAE609 and M37 showed a shift of the protonated molecular ion from *m/z* 390 to MD<sup>+</sup> at *m/z* 394 in KAE609 and from *m/z* 390 to MD<sup>+</sup> at *m/z* 393 in M37, suggesting that there are three exchangeable hydrogen atoms in KAE609 and only two exchangeable hydrogen atoms in M37 (data not shown).

A comparison of <sup>1</sup>H spectra acquired for the rat feces-derived sample of M37 with KAE609 showed that M37 has five aromatic protons with similar coupling patterns as were observed for KAE609 (Fig. 3). The chemical shifts of the M37 aromatic protons are different from KAE609, with the aromatic singlet of M37 at 7.29 ppm showing the most significant chemical shift difference relative to the parent molecule. These NMR spectra suggest that no metabolism occurred on the aromatic rings of KAE609 during biotransformation to M37.

In the aliphatic region of the M37 spectrum, a multiplet was observed at 4.95 ppm arising from the methine of M37 at H-8. The methyl group (1.28 ppm) and the methylene protons (2.59, 3.09 ppm) were identified from correlation spectroscopy (COSY). Both showed COSY correlations to the H-8 proton. The chemical shift of the methine proton suggested that it was still connected to nitrogen as in KAE609's structure.

The most significant difference between M37 and the parent drug spectra is an additional singlet observed at 5.84 ppm (<sup>1</sup>H) in the

metabolite spectrum. Acquisition of the one-dimensional nuclear Overhauser effect spectroscopy spectrum demonstrated that the proton at 5.84 ppm has a through-space correlation to the methyl doublet at 1.28 ppm and the aromatic singlet at 7.50 ppm, indicating that it is close to the chlorobenzene moiety. In addition, the aromatic singlet at 7.50 ppm showed a nuclear Overhauser effect correlation to the NH proton (H14) at 9.21 ppm. These observations suggest that the spiro ring of KAE609 has expanded and rearranged. Based on the NMR, exchangeable hydrogen atoms, and MS/MS results, a structure was proposed for M37 as shown in Fig. 3. Because of the limited quantity of samples, further structure confirmation via heteronuclear multiple bond correlation (HMBC) experiments could not be performed. The structure of M37 was further confirmed by chemical synthesis.

### Structural Characterization of M18 by LC-MS/MS and NMR

M18 ([MH]<sup>+</sup> = 388) was an oxidative metabolite of KAE609 with a net decrease of 2 Da in mass. The product ion spectrum showed fragment ions at *m/z* 359 (loss of ethyl group) and 324 (loss of Cl radical from *m/z* 359).

<sup>1</sup>H spectra of the metabolite M18 and KAE609 are shown in Fig. 4. In the aliphatic region of the M18 spectrum, a multiplet was observed at 5.63 ppm corresponding to a methine proton H-8. The methyl group (1.21 ppm) and the methylene protons (3.20 and 3.38 ppm) were identified from COSY spectrum.

<sup>1</sup>H spectrum of M18 showed five aromatic protons with coupling patterns similar to the parent compound. However, the chemical shifts of M18's aromatic protons differed from KAE609, with H-1 showing the most significant difference. The methine singlet observed in M37 is absent. The MS results showed that M18 is 2 Da less than that of M37 and has one less exchangeable proton compare with M37. The LC-MS and NMR results suggest that M18 appears to be derived from previously identified M37. The structure of M18 was also confirmed by chemical synthesis.

### Structural Characterization of M23 by LC-MS/MS and NMR

M23 ([MH]<sup>+</sup> = 404) was a hydroxylated metabolite of M18 with a net increase of 14 Da in mass versus KAE609. The product ion spectra of M23 showed fragment ions at *m/z* 375 and 340, which were 16 Da higher in mass than fragment ions from M18, supporting the assignment.

In the H/D exchange experiment, the full-scan mass spectrum of M18 and M23 showed a shift of the protonated molecular ion from *m/z* 388 to MD<sup>+</sup> at *m/z* 390 for M18 and from *m/z* 404 to MD<sup>+</sup> at *m/z* 407 for M23, consistent with the assignment that M23 was a hydroxylated metabolite of M18 (data not shown).

High-resolution MS data of compound 3, generated biocatalytically, suggested a molecular formula of C<sub>19</sub>H<sub>12</sub>Cl<sub>2</sub>FN<sub>3</sub>O<sub>2</sub> or one oxygen atom more than KAE609 and two hydrogen atoms less. Compared with the <sup>1</sup>H-NMR spectrum of KAE609, the data of compound 3 showed only four aromatics protons (Table 2). The presence of two aromatic protons (H-10 and H-13) which showed coupling to <sup>19</sup>F suggested that the 6-chloro-5-fluoro-indole ring was intact. However, the 5-chloro-indolone coupling pattern was no longer present. Instead, two singlets were observed at 6.20 and 8.25 ppm. There was no correlation in COSY and total correlation spectroscopy between these two protons. A rotational frame nuclear Overhauser effect spectroscopy correlation was observed between the NH-14 of the 6-chloro-5-fluoro-indole and the singlet at 8.25 ppm (H-1). The detailed rotational frame nuclear Overhauser effect spectroscopy correlation spectrum of compound 3 can be found in

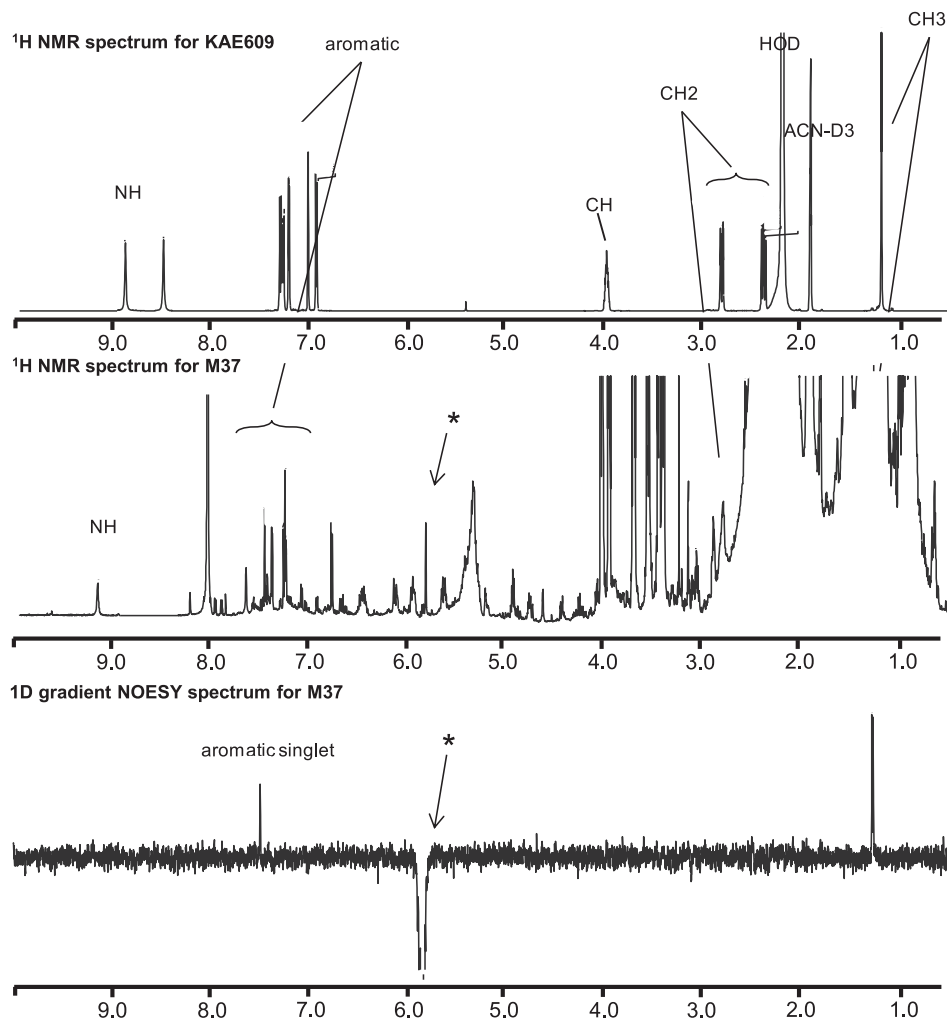
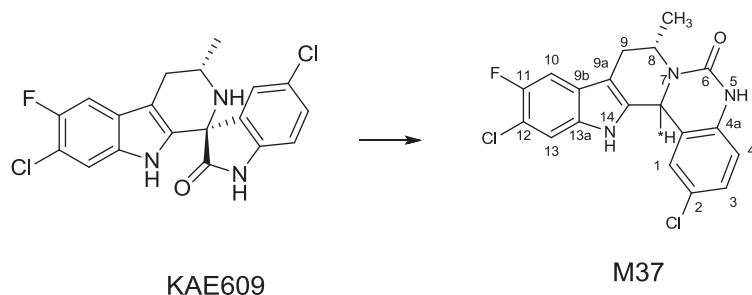


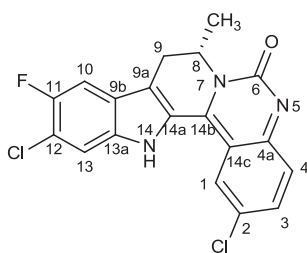
**Fig. 3.** <sup>1</sup>H NMR spectra for KAE609 and M37 and NOESY spectrum for M37 isolated from rat fecal extracts after dosing of [<sup>14</sup>C]KAE609. <sup>1</sup>H Spectra of M37 enriched from rat feces and authentic KAE609 were compared (top two panels). The one-dimensional gradient NOESY spectrum was acquired after the proton (at 5.84 ppm, designated with an asterisk) was irradiated to reveal the space correlations between the aromatic singlet and methyl protons (bottom panel). All samples were dissolved in acetonitrile-*d*<sub>3</sub>. NOESY, nuclear Overhauser effect spectroscopy.

Supplemental Fig. 7. The proton at 6.20 ppm (H-4) showed an HMBC correlation with the carbons C-2 and C-14c, confirming the position on C-4. The chemical shift of C-3 at 174.1 ppm, extracted from the HMBC experiment (H-1 to C-3) indicated that a hydroxylation had occurred on position 3. The aliphatic CH resonance at 5.33 ppm (H-8) showed a HMBC correlation to C-14b at 143.0 ppm. This chemical shift indicated that C-14b was now sp<sup>2</sup> hybridized in contrast with KAE609, where it was sp<sup>3</sup>. This suggested that the ring of the spiro had opened between C-14b and C-6 and rearranged. The chemical shift of H-8 indicated the formation of quinazolinone moiety. This was further supported by the down field shift compared with the

KAE609 spectrum due to the anisotropy cone effect of the neighboring C=O.

#### NMR Analysis of Enriched M23 from Fecal Samples Compared with Authentic Compound 3 from Bioreactions

Analysis of the <sup>1</sup>H spectra revealed that the enriched M23-containing rat fecal sample included a chemical species with protons of the same chemical shifts and coupling patterns as that of compound 3: H-1, H-4, H-10, and H-13. In addition, <sup>1</sup>H signals corresponding to H-4 for both the compound 3 and M23 samples appeared as broad singlets, suggesting that the putative M23 H-4 proton is adjacent to a heteroatom



62224N1G100067\_KAEM37\_1.001.001.1r.esp

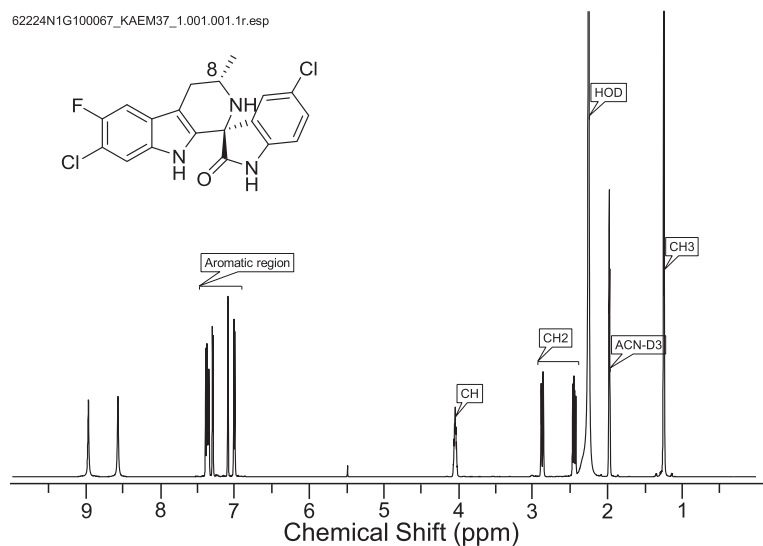
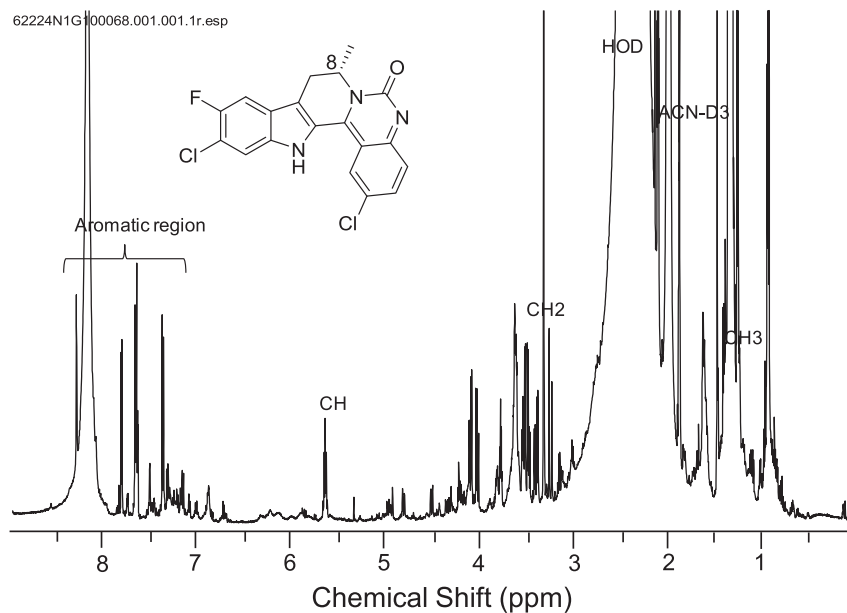


**Fig. 4.**  $^1\text{H}$  NMR spectra for KAE609 and M18 isolated from rat hepatocytes.  $^1\text{H}$  spectra of M18 enriched from rat hepatocyte incubations and authentic KAE609 were compared. Both samples were dissolved in acetonitrile- $d_3$ .

62224N1G100068.001.001.1r.esp



bearing an exchangeable proton. The difference of proton chemical shift of H-4 [6.20 ppm from compound 3 (Table 2) and 5.95 ppm from M23 from fecal pool] may be attributed to a difference in sample concentration or pH due to the proximity of the hydroxyl at C-3.

The aliphatic region of the M23-containing sample  $^1\text{H}$  spectrum was crowded with signals corresponding to matrix components. Therefore,

to obtain a partially deconvoluted picture of the  $^1\text{H}$ - $^1\text{H}$  spin systems in this region, a DQF-COSY spectrum was acquired. The DQF-COSY spectrum shows a spin system with chemical shifts and coupling patterns matching the  $\text{CH}_3\text{-CH-CH}_2$  moiety in compound 3. Comparison of NMR spectra of M23 derived from a rat fecal pool and compound 3 from biosynthesis can be found in Supplemental Fig. 8.

TABLE 2

<sup>1</sup>H- and <sup>13</sup>C assignments and important HMBC correlations of compound 3 isolated from biosynthesis with recombinant human CYP1A2 in *E. coli*

Coupling constants are given in Hertz.

Atom Number <sup>a</sup>	Compound 3		
	<sup>1</sup> H NMR	<sup>13</sup> C Shift <sup>b</sup>	HMBC Correlations
1	8.25	s	128.3
2			130.4
3			174.1
3-OH	9.76	br s	
4	6.20	br s	101.1
4a			144.8
6			n.o. <sup>c</sup>
8	5.33	qd, 6.6, 6.1	48.7
8-Me	1.13	d, 6.6	16.5
9R	3.27	dd, 16.6, 6.4	25.1
9S	3.13	d, 16.8	
9a			122.4
9b			125.2
10	7.59	d, 9.2	106.6
11			154.1
12			121.1
13	7.77	d, 6.4	114.0
13a			137.8
14	10.44	br s	
14a			127.0
14b			143.0
14c			102.5

br, broad; d, doublet; q, quartet; s, singlet.

<sup>a</sup>For atom numbering, see Figure 5.

<sup>b</sup>The <sup>13</sup>C shifts were extracted from heteronuclear single quantum coherence and HMBC correlation peaks.

<sup>c</sup>Not observed in the HMBC experiment.

### In Vitro Metabolism of KAE609 and M18 by Human Recombinant CYP Enzymes

To examine the roles of specific CYP enzymes involved in the metabolism of [<sup>14</sup>C]KAE609, several recombinant CYP enzymes were tested. The recombinant human CYP enzymes found capable of oxidative metabolism of KAE609 were CYP2C9, CYP2C19, CYP3A4, and CYP3A5 (Fig. 5A). M37 and M18 were among the metabolites identified from the incubations. However, M23 was not detected in any of the incubations with CYP enzymes.

As mentioned previously, the structure of M18 was proposed based on NMR analysis and later confirmed by chemical synthesis (compound 2). Thus, compound 2 (M18) was used as a substrate in in vitro incubation to determine the CYP enzymes involved in the oxidative metabolism of M18. M14 was the major metabolite generated in incubations with all recombinant CYP enzymes tested. Trace levels of M23 were detected in incubations with CYP1A1, CYP1A2, and CYP1B1 (Fig. 5B).

### Proposed Metabolite Pathways of [<sup>14</sup>C]KAE609 in Rats and Dogs

Metabolic pathways of KAE609 in rats and dogs are summarized in Fig. 6. KAE609 underwent C-C bond cleavage, followed by a 1,2-acyl shift and ring expansion to form M37, which underwent oxidation to form the colored metabolite M18, which was further hydroxylated to form another colored metabolite M23. M37 was the major metabolite in rat feces, whereas M23 was the major metabolite in dog feces. KAE609 also underwent oxidation to M40 and M20.1 with 2 mass units lower than that of KAE609 and one metabolite (M48) with 4 mass units lower than that of KAE609. KAE609 was directly hydroxylated to form two metabolites (M26 and M34). Metabolites (M40, M20.1, and M48) were further hydroxylated to several metabolites (M14, M20, M21.2, M24, M36, M39, M44, and M46). Several glucuronides were also identified in bile from the bile

duct-cannulated rat, with the total accounting for approximately 19% of the oral dose (data not shown).

### Discussion

KAE609 is an antimalarial agent that is progressing through clinical development, providing a potentially new cure to combat malaria drug resistance concerns (Rottmann et al., 2010; Meister et al., 2011; Spillman et al., 2013). To facilitate the understanding of metabolism and disposition of KAE609 in humans, ADME studies in nonclinical species and across species in vitro metabolism studies were conducted.

After intravenous or oral dosing of [<sup>14</sup>C]KAE609, mass balance was achieved in both rats and dogs. The radioactivity was primarily excreted via biliary or fecal pathways (>93% of dose recovered in feces). After oral dosing, KAE609 was well absorbed and extensively metabolized in rats and dogs. KAE609 showed low clearance, moderate volume distribution, and a long *t*<sub>1/2</sub> in rats and dogs. The most abundant radioactive component in rat and dog plasma was KAE609, accounting for approximately 75%–84% of the total radioactivity in plasma. M18 was identified to be the major circulating metabolite in rats and dogs, accounting for approximately 10%–19% of the total radioactivity in plasma. M37 was the major metabolite in rat feces, whereas M23 was the major metabolite in dog feces. Despite M23 being the major metabolite in dog feces, M23 was not detected in the circulation in either rat or dog plasma after intravenous or oral dosing of KAE609.

As mentioned previously, M23 was identified as a human metabolite based on in vitro incubations of KAE609 with hepatocytes. M23 was not detected in rat and dog plasma from ADME studies, suggesting that M23 may pose exposure coverage concerns if M23 is in the circulation of humans. Therefore, to determine whether M23 is present in human plasma, we conducted metabolite identification by LC-MS/MS using the plasma from the first-in-human study. M23 was confirmed to be present in human plasma (data not shown). Consequently, we decided to conduct a human ADME study to better define the exposure of M23 relative to total radioactivity exposure in plasma (Huskey et al., submitted manuscript). Our findings showed that M23 accounted for approximately 12% of total radioactivity exposure in human plasma. Based on the recommendation of Metabolites in Safety Testing and International Conference on Harmonisation guidance (see U.S. Food and Drug Administration 2008, 2010, and 2012 guidance, available at <http://www.fda.gov/cder/guidance/index.htm> and <http://www.fda.gov/Drugs/GuidanceComplianceRegulatoryInformation/Guidances/default.htm>), safety testing of M23 in nonclinical species is planned accordingly.

To complement the aforementioned metabolite in safety testing, it was critical to elucidate the structures of the metabolites involved in the pathway leading to M23. KAE609, a spiroindolone derivative, undergoes an unusual C-C bond cleavage, followed by a 1,2-acyl shift to form a ring expansion product M37. This isomerization and rearrangement reaction was catalyzed by CYP3A4 and the mechanism of this novel biotransformation reaction is proposed in Fig. 7. KAE609 undergoes oxidation by a single electron transfer to form a radical cation, followed by C-C bond cleavage to form an isocyanate radical cation intermediate. The isocyanate radical cation is reduced by a single electron transfer, followed by protonation. Nucleophilic attack by the amine on the carbonyl carbon of the isocyanate leads to ring closure to form M37. A similar mechanism via a one-electron oxidized intermediate has been proposed for the nonoxidative decarboxylation of *N*-alkyl-*N*-phenylglycines by horseradish peroxidase in the absence of H<sub>2</sub>O<sub>2</sub> and O<sub>2</sub> (Totah and Hanzlik, 2002, 2004).

As mentioned previously, structures of M37 and M18 were proposed based on a combination of LC-MS/MS, exchangeable hydrogen atoms,

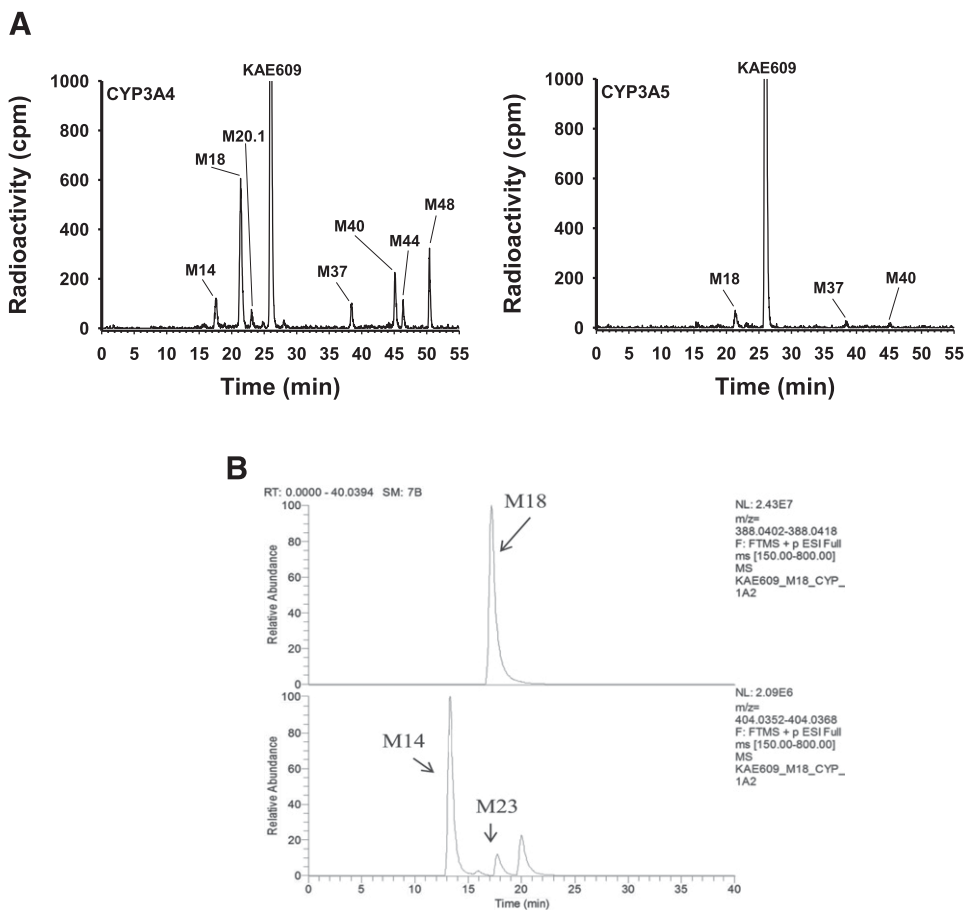


**Fig. 5.** In vitro metabolism of KAE609 and compound 2 (M18) with human recombinant CYP enzymes. [ $^{14}\text{C}$ ] KAE609 ( $44\ \mu\text{M}$ ) or compound 2 (M18;  $50\ \mu\text{M}$ ) was incubated with a panel of human recombinant CYP enzymes ( $100\ \text{pmol CYP}\cdot\text{mL}^{-1}$ ) or control microsomes in the presence of NADPH. The reactions were incubated at  $37^\circ\text{C}$  for 30 minutes and quenched with an equal volume of cold acetonitrile and the products were analyzed by LC-MS/MS and/or radioactivity monitoring. The assignment of M23 in the extracted ion chromatogram was based on MS/MS analysis. (A) Incubations with CYP2C9 and CYP2C19 showed same results as that with CYP3A5. (B) Incubations of compound 2 with CYP1A1 and CYP1B1 showed the same results as that with CYP1A2.

and NMR analyses. However, structural assignment for M23 was not achievable due to an insufficient quantity of sample isolated from rat feces. Therefore, our strategy was to use in vitro incubations to facilitate the M23 structural assignment. Specifically, we incubated M18 with a panel of human recombinant CYP enzymes and identified CYP1A1, CYP1A2, and CYP1B1 as responsible for the formation of M23 from M18. We then pursued this CYP-catalyzed reaction using recombinant human CYP1A2 (whole-cell biotransformation with genetically modified *E. coli*) to generate approximately 1 mg of M23 for structural elucidation and evaluation of pharmacological activity.

The metabolic pathways of KAE609 are proposed (Fig. 6) based on metabolite profiling and characterization efforts conducted using LC-MS/MS and NMR analyses of metabolites. KAE609, a spiroindolone derivative, undergoes an unusual C-C bond cleavage, followed by a 1,2-acyl shift to form a ring expansion product M37. This novel biotransformation reaction was primarily catalyzed by CYP3A4. M37 was subsequently oxidized to M18 by CYP3A4 and hydroxylated to M23 by CYP1A1, CYP1A2, and CYP1B1. All three metabolites had conjugated systems of double bonds, which imparted their characteristic color. As expected, M37 was colorless having two isolated conjugation systems. With only one additional double bond, M18 and M23 gained an elongated conjugation system, resulting in M18 with an orange yellow color and M23 with a yellow color. The proposed structures of the three metabolites were chemically synthesized and thereby confirmed their structural assignments. They were found to be pharmacologically inactive since the spiroindolone core, required for pharmacological activity, was lost during biotransformation. Moreover, safety evaluation of M23 showed it to be negative in the AMES test and in the human lymphocyte chromosomal aberration test.

It is interesting that M23 was the major metabolite in dog feces and a minor metabolite in rat feces; however, M23 was not in either rat or dog plasma. In contrast, M23 was the major metabolite in human plasma and feces (Huskey et al., submitted manuscript). Apparently, M23 was generated enzymatically in the liver from KAE609 via intermediates M37 and M18 in all three species. However, the distribution of these three metabolites was different in rats and dogs versus humans. Thus, we hypothesized that species differences in transporters dictate the distribution of M23 to blood (humans) or excretion into biliary or fecal pathways (rats, dogs, and humans).

The prediction of circulating metabolites in humans and why certain metabolites circulate are topics of interest in drug metabolism research, as discussed in several publications (Anderson et al., 2009; Dalvie et al., 2009; Smith and Dalvie, 2012). When species differences are observed in the disposition of metabolites, as was the case for metabolite M23 of KAE609, it may lead to the necessary safety evaluation of metabolites depending on their exposure in humans (see U.S. Food and Drug Administration 2008, 2010, and 2012, guidance available at <http://www.fda.gov/cder/guidance/index.htm> and <http://www.fda.gov/Drugs/GuidanceComplianceRegulatoryInformation/Guidances/default.htm>). Thus, it is crucial to proactively address such concerns during early development to avoid potential delays in new drug application approval.

#### Acknowledgments

The authors thank Dr. Francis Tse for constructive discussion and continued encouragement and support, Dr. Robert Hanzlik (University of Kansas) for insightful and constructive discussion for the mechanism of the novel biotransformation reaction, Dr. Bryan Yeung for encouragement and insightful suggestions in the chemical synthesis of metabolites, and Dr. Andreas

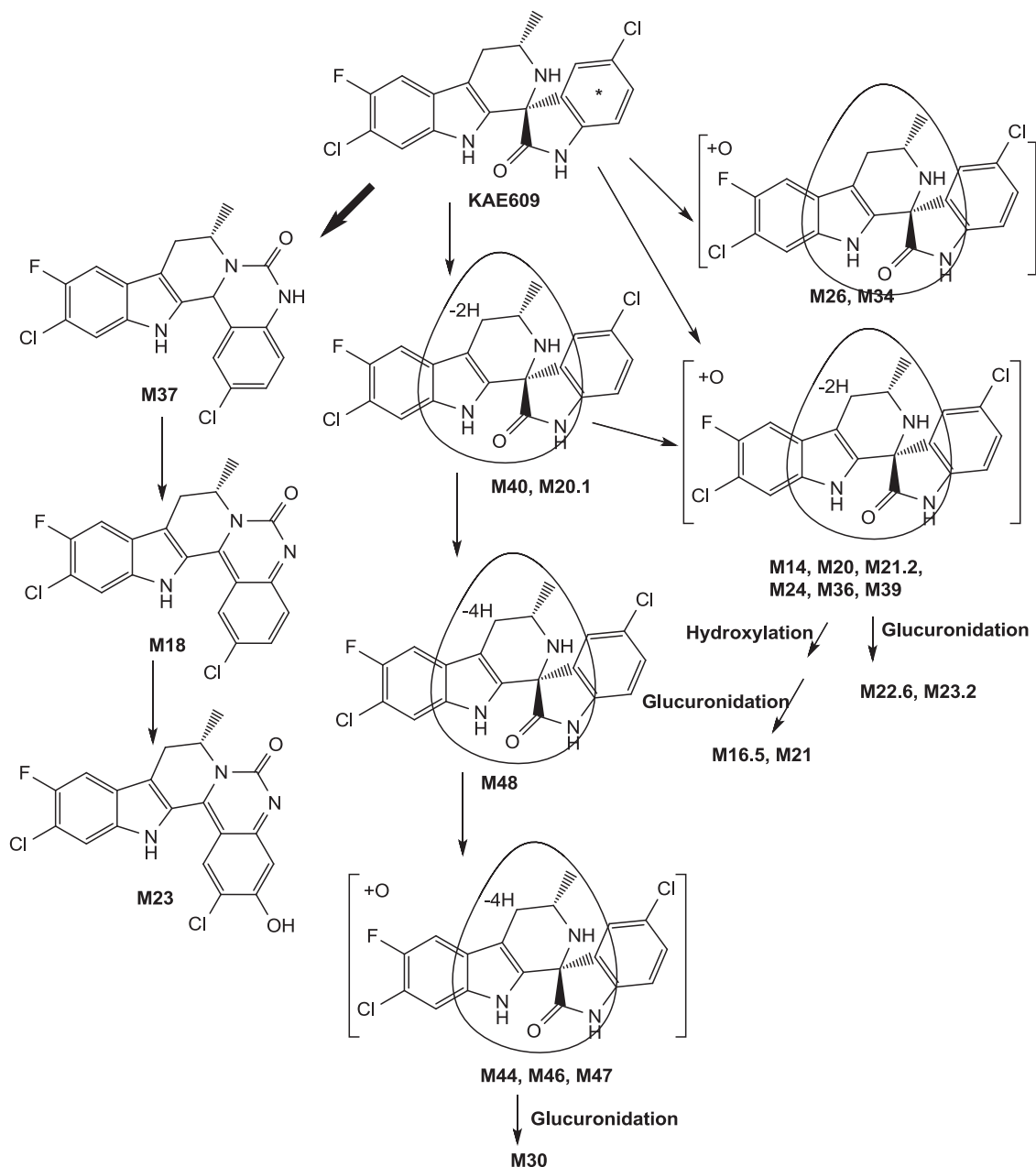


**Fig. 6.** Proposed metabolic pathways of KAE609 in rats and dogs. Structures of M37, M18, and M23 were characterized by LC-MS/MS and NMR analyses and further confirmed by chemical synthesis. However, the assignments of remaining metabolites were only based on LC-MS/MS analysis. Several glucuronides (M16.5, M21, M22.6, M23.2, and M30) were identified in bile from bile duct-cannulated rats.

Fredenhagen for expert opinions and practical suggestions. The authors also thank Dr. Zhigang Jian for synthesis of [ $^{14}\text{C}$ ]KAE609, Dr. Amy Wu and Mr. Lawrence Jones for purification and analytical certification of

[ $^{14}\text{C}$ ]KAE609, Dr. Ziping Yang and Ms. Cindy Chen for quantification of KAE609 in rat and dog plasma, and Lolita Rodriguez for metabolic profiling of KAE609 in biological matrices from rats.

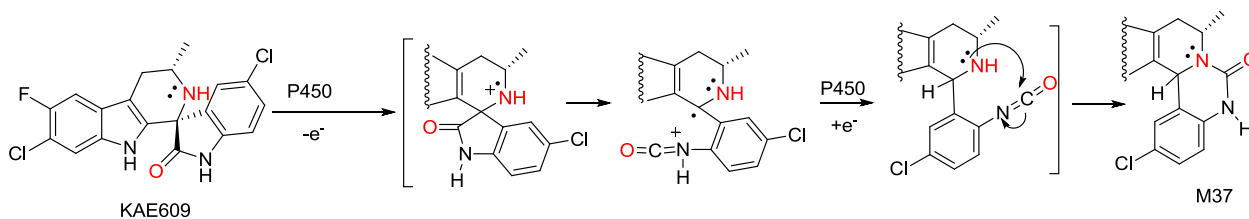


**Fig. 7.** Proposed mechanism for the formation of M37. The structure of M37 was characterized by LC-MS/MS and NMR analyses and further confirmed by chemical synthesis.

### Authorship Contributions

*Participated in study design:* Huskey, Zhang, Favara, He.

*Conducted experiments:* Zhu, Forseth, Gu, Simon, Eggimann, Vargas, Li, Wang, Zhang, Favara.

*Performed data analysis:* Huskey, Zhu, Lin, Forseth, Gu, Eggimann, Kittelmann, Luneau, Einolf.

*Wrote or contributed to the writing of manuscript:* Huskey, Forseth, Simon, Eggimann, Kittelmann, Luneau, Mangold.

### References

- Anderson S, Luffer-Atlas D, and Knadler MP (2009) Predicting circulating human metabolites: how good are we? *Chem Res Toxicol* **22**:243–256.
- Baillie TA (2008) Metabolism and toxicity of drugs. Two decades of progress in industrial drug metabolism. *Chem Res Toxicol* **21**:129–137.
- Baillie TA, Cayen MN, Fouda H, Gerson RJ, Green JD, Grossman SJ, Klunk LJ, LeBlanc B, Perkins DG, and Shipley LA (2002) Drug metabolites in safety testing. *Toxicol Appl Pharmacol* **182**:188–196.
- Carter TE, Boulter A, Existe A, Romain JR, St Victor JY, Mulligan CJ, and Okech BA (2015) Artemisinin resistance-associated polymorphisms at the K13-propeller locus are absent in *Plasmodium falciparum* isolates from Haiti. *Am J Trop Med Hyg* **92**:552–554.
- Dalvie D, Obach RS, Kang P, Prakash C, Loi CM, Hurst S, Nedderman A, Goulet L, Smith E, and Bu HZ, et al. (2009) Assessment of three human in vitro systems in the generation of major human excretory and circulating metabolites. *Chem Res Toxicol* **22**:357–368.
- Haque U, Glass GE, Haque W, Islam N, Roy S, Karim J, and Noedl H (2013) Antimalarial drug resistance in Bangladesh, 1996–2012. *Trans R Soc Trop Med Hyg* **107**:745–752.
- Hott A, Casandra D, Sparks KN, Morton LC, Castaneres G-G, Rutter A, and Kyle DE (2015) Artemisinin-resistant *Plasmodium falciparum* parasites exhibit altered patterns of development in infected erythrocytes. *Antimicrob Agents Chemother* **59**:3156–3167.
- Huskey SE, Zhu C-Q, Fredenhagen A, Kühnöl J, Lumeaux A, Jian Z, Yang Z, Mia Z, Yang F, Jain JP, Sunkara G, Mangold JB and Stein DS (2016) KAE609 (Cipargamin), a new spiroindolone agent for the treatment of malaria: Evaluation of the Absorption, Distribution, Metabolism and Excretion of a single oral 300 mg dose of [<sup>14</sup>C]KAE609 in healthy male subjects *Drug Metab Dispos* (submitted for peer review)
- Kittelmann M, Kuhn A, Riepp A, Kühnöl J, Fredenhagen A, Oberer L, Ghisalba O, and Luetz S (2012) Recombinant human cytochrome P450 enzymes expressed in *Escherichia coli* as whole cell biocatalysts: preparative synthesis of oxidized metabolites of an mGlu5 receptor antagonist, in *Practical Methods for Biocatalysis and Biotransformations 2* (Whittall J and Sutton PW eds.) pp 138–146, John Wiley & Sons, Ltd., Chichester, UK.

- Leong FJ, Li R, Jain JP, Lefèvre G, Magnusson B, Diagana TT, and Pertel P (2014) A first-in-human randomized, double-blind, placebo-controlled, single- and multiple-ascending oral dose study of novel antimalarial spiroindolone KAE609 (Cipargamin) to assess its safety, tolerability, and pharmacokinetics in healthy adult volunteers. *Antimicrob Agents Chemother* **58**:6209–6214.
- Meister S, Plouffe DM, Kuhen KL, Bonamy GM, Wu T, Barnes SW, Bopp SE, Borboa R, Bright AT, and Che J, et al. (2011) Imaging of *Plasmodium* liver stages to drive next-generation antimalarial drug discovery. *Science* **334**:1372–1377.
- Na-Bangchang K and Karbwang J (2013) Emerging artemisinin resistance in the border areas of Thailand. *Expert Rev Clin Pharmacol* **6**:307–322.
- Rottmann M, McNamara C, Yeung BK, Lee MCS, Zou B, Russell B, Seitz P, Plouffe DM, Dharia NV, and Tan J, et al. (2010) Spiroindolones, a potent compound class for the treatment of malaria. *Science* **329**:1175–1180.
- Smith DA and Dalvie D (2012) Why do metabolites circulate? *Xenobiotica* **42**:107–126.
- Smith DA and Obach RS (2009) Metabolites in Safety Testing (MIST): considerations of mechanisms of toxicity with dose, abundance, and duration of treatment. *Chem Res Toxicol* **22**:267–279.
- Spillman NJ, Allen RJW, McNamara CW, Yeung BKS, Winzeler EA, Diagana TT, and Kirk K (2013) Na<sup>(+)</sup> regulation in the malaria parasite *Plasmodium falciparum* involves the cation ATPase PfATP4 and is a target of the spiroindolone antimalarials. *Cell Host Microbe* **13**:227–237.
- Totah RA and Hanzlik RP (2002) Non-oxidative decarboxylation of glycine derivatives by a peroxidase. *J Am Chem Soc* **124**:10000–10001.
- Totah RA and Hanzlik RP (2004) Oxidative and nonoxidative decarboxylation of N-Alkyl-N-phenylglycines by horseradish peroxidase. Mechanistic switching by varying hydrogen peroxide, oxygen, and solvent deuterium. *Biochemistry* **43**:7907–7914.
- White NJ, Pukrittayakamee S, Phyo AP, Rueangweerayut R, Nosten F, Jittamala P, Jeeyapant A, Jain JP, Lefèvre G, and Li R, et al. (2014) Spiroindolone KAE609 for *falciparum* and vivax malaria. *N Engl J Med* **371**:403–410.
- Witkowski B, Khim N, Chim P, Kim S, Ke S, Kloeung N, Chy S, Duong S, Leang R, and Ringwald P, et al. (2013) Reduced artemisinin susceptibility of *Plasmodium falciparum* ring stages in western Cambodia. *Antimicrob Agents Chemother* **57**:914–923.
- Yeung BK, Zou B, Rottmann M, Lakshminarayana SB, Ang SH, Leong SY, Tan J, Wong J, Keller-Maerki S, and Fischli C, et al. (2010) Spiroindolone β-carbolines (spiroindolones): a new class of potent and orally efficacious compounds for the treatment of malaria. *J Med Chem* **53**:5155–5164.

---

**Address correspondence to:** Su-Er Wu Huskey, Drug Metabolism and Pharmacokinetics, Novartis Institutes for BioMedical Research, One Health Plaza, East Hanover, NJ 07936-1080. E-mail: Su.huskey@novartis.com

---